A GENERALIZED SPACE MAPPING TABLEAU APPROACH TO MICROWAVE DEVICE MODELING

J.W. Bandler, N.Georgieva, M.A. Ismail, J.E. Rayas-Sánchez and Q.J. Zhang

SOS-99-18-R

June 1999

(Full paper)

A GENERALIZED SPACE MAPPING TABLEAU APPROACH TO DEVICE MODELING

John W. Bandler, *Fellow*, *IEEE,* N. Georgieva, *Member*, *IEEE*, Mostafa A. Ismail, *Student Member*, *IEEE*, José E. Rayas-Sánchez, *Senior Member*, *IEEE,* and Qi-Jun Zhang, *Senior Member*, *IEEE*

Abstract A comprehensive framework to engineering device modeling which we call Generalized Space Mapping (GSM) is introduced. GSM permits many different practical implementations. As a result the accuracy of available empirical models of microwave devices can be significantly enhanced. We present three fundamental illustrations: a basic Space Mapping Super Model (SMSM), Frequency-Space Mapping Super Model (FSMSM) and Multiple Space Mapping (MSM). Two variations of MSM are presented: MSM for Device Responses (MSMDR) and MSM for Frequency Intervals (MSMFI). We also present novel criteria to discriminate between coarse models of the same device. The SMSM, FSMSM and MSM concepts have been verified on several modeling problems, typically utilizing a few relevant full-wave EM simulations. This paper presents four examples, a microstrip line, a microstrip right angle bend, a microstrip step junction and a microstrip shaped T-junction, yielding remarkable improvement within regions of interest.

I. INTRODUCTION

We generalize the Space Mapping (SM) [1], the Frequency Space Mapping (FSM) [2] and the Multiple Space Mapping (MSM) [3] concepts to build a new engineering device modeling framework.

This work was supported in part by the Natural Sciences and Engineering Research Council of Canada under Grants OGP0007239, STP0201832, Com Dev, Nanowave Technologies and through the Micronet Network of Centres of Excellence. J.E. Rayas-Sánchez is funded by CONACYT (Consejo Nacional de Ciencia y Tecnología, Mexico), as well as by ITESO (Instituto Tecnológico y de Estudios Superiores de Occidente, Mexico). N. Georgieva is supported by an NSERC Postdoctorate Fellowship.

J.W. Bandler, N. Georgieva, M.A. Ismail and J.E. Rayas-Sánchez are with the Simulation Optimization Systems Research Laboratory and the Department of Electrical and Computer Engineering, McMaster University, Hamilton, Ontario, Canada L8S 4K1.

J.W. Bandler is also with Bandler Corporation, P.O. Box 8083, Dundas, Ontario, Canada L9H 5E7.

Q.J. Zhang is with the Department of Electronics, Carleton University, 1125 Colonel By Drive, Ottawa, Canada K1S 5B6.

This framework is flexible enough to permit a number of implementable special cases. The important observation that we make is that the methodology closely follows sound engineering design practice. Our contribution is a mathematical formulation suitable for device modeling and a clear practical interpretation. We refer to the concept generically as the Generalized Space Mapping (GSM) concept.

The mathematical formulation of the GSM framework is not complicated. It is expected to be useful in assisting designers to evaluate the accuracy of empirical models and/or to discriminate between them. Intuitively meaningful quantitative measures of model accuracy can be developed through careful interpretations of GSM.

Significant enhancement of the accuracy of available empirical models of microwave devices can be realized. Three fundamental cases are presented: Space Mapping Super Model (SMSM) which maps designable device parameters, a basic Frequency-Space Mapping Super Model (FSMSM) which maps the frequency variable as well as the designable device parameters and Multiple Space Mapping (MSM). We present two variations of MSM: MSM for Device Responses (MSMDR) and MSM for Frequency Intervals (MSMFI). In MSMDR we divide the set of device responses into a number of sub-responses and establish a separate mapping for each sub-response. In MSMFI we divide the frequency range of interest into a number of intervals and establish a separate mapping for each interval. Two algorithms to implement MSMDR and MSMFI are also presented.

Two model types are usually defined in the SM process [1]: a "coarse" model, typically an empirical model, and a "fine" model, typically a full-wave EM simulator. Empirical models of microwave devices behave well in certain parameter and frequency regions. They are computationally very fast and are preferred for initial design purposes over accurate but CPU intensive full-wave EM simulators.

The basic SMSM, FSMSM and MSM concepts have been validated on a number of modeling problems, typically utilizing a few relevant full-wave EM simulations. This paper presents four illustrations, a microstrip line, a microstrip right angle bend, a microstrip step junction and a microstrip shaped T-junction, yielding remarkable improvement within the regions of interest.

II. THE GSM CONCEPT

Consider a microwave device with physical parameters represented by an *n*-dimensional vector $\boldsymbol{x}_f$. In general, the response $\boldsymbol{R}_c(\boldsymbol{x}_f, ?)$ produced by the coarse model deviates from the response $\boldsymbol{R}_f(\boldsymbol{x}_f, ?)$ produced by an EM simulator, where $?$ is the frequency variable. Therefore, the aim is to find a mapping from the fine model parameters and the frequency variable to a new set of parameters and a new frequency variable so that the responses of the two models match. Mapping the space parameters was introduced by Bandler *et al*. [1] and mapping the frequency variable was introduced later in [2]. The mapped coarse model parameters are represented by an *n*-dimensional vector $\boldsymbol{x}_c$ and the mapped frequency variable is represented by $?_c$. We call this scheme Frequency-Space Mapping Super Model (FSMSM) as illustrated in Fig. 1. A special case of FSMSM is to map only the fine model parameters and leave the frequency variable unchanged. We call this the Space Mapping Super Model (SMSM), as illustrated in Fig. 2. Once FSMSM or SMSM are established the enhanced coarse model (see Fig. 3) can be utilized for analysis or design purposes. We will compare the FSMSM and SMSM in one of the examples.

The mapping relating the fine model parameters and frequency to the coarse model parameters and frequency is given by

$$[\boldsymbol{x}_c \quad ?_c]^T = \boldsymbol{P}(\boldsymbol{x}_f, ?) \tag{1}$$

Or, in matrix form, assuming a linear mapping,

$$\begin{bmatrix} \boldsymbol{x}_c \\ ?_c^{-1} \end{bmatrix} = \begin{bmatrix} \boldsymbol{c} \\ d \end{bmatrix} + \begin{bmatrix} \boldsymbol{B} & \boldsymbol{s} \\ \boldsymbol{t}^T & s \end{bmatrix} \begin{bmatrix} \boldsymbol{x}_f \\ ?^{-1} \end{bmatrix} \tag{2}$$

where $\{\boldsymbol{c}, \boldsymbol{B}, \boldsymbol{s}, d, \boldsymbol{t}, s\}$ are the parameters characterizing the mapping $\boldsymbol{P}$. The constant vectors $\boldsymbol{c}, \boldsymbol{s}, \boldsymbol{t}$ are *n*-dimensional, $\boldsymbol{B}$ is an *n* x *n* matrix and d, s are scalar. In (2) we notice that we map the inverse of the frequency (which is proportional to the wavelength) instead of the frequency itself. This has produced better results in all the models we considered than mapping the frequency directly. It can be also justified

by the fact that in most microwave structures shrinking the structure would lead to a shift of its spectral characteristics to higher frequencies (shorter wavelengths).

The mapping parameters in (2) can be evaluated by solving the optimization problem

$$\min_{\boldsymbol{c},\boldsymbol{B},\boldsymbol{s},d,\boldsymbol{t},s} \left\| \begin{bmatrix} \boldsymbol{e}_1^T & \boldsymbol{e}_2^T & \cdots & \boldsymbol{e}_N^T \end{bmatrix}^T \right\| \tag{3}$$

subject to suitable constraints, where $\| \ \|$ is a suitable norm, N is the total number of fine model simulations and $\boldsymbol{e}_k$ is an error vector given by

$$\boldsymbol{e}_k = \boldsymbol{R}_f(\boldsymbol{x}_{f_i}, ?_j) - \boldsymbol{R}_c(\boldsymbol{x}_c, ?_c), \tag{4a}$$

$$\begin{bmatrix} \boldsymbol{x}_c & ?_c \end{bmatrix}^T = \boldsymbol{P}(\boldsymbol{x}_{f_i}, ?_j) \tag{4b}$$

with

$$i = 1, \cdots, B_p \tag{5a}$$

$$j = 1, \cdots, F_p \tag{5b}$$

$$k = j + (i-1)F_p \tag{5c}$$

where B_p is the number of base points and F_p is the number of frequency points per frequency sweep. The total number of fine model simulations is $N = B_p\ F_p$. The constraints we impose on the mapping parameters are that the mapping parameters should be as close as possible to the parameters corresponding to a unit mapping $\boldsymbol{x}_c = \boldsymbol{x}_f$ and $?_c = ?$ which corresponds to $\{\boldsymbol{c} = \boldsymbol{0}, \boldsymbol{B} = \boldsymbol{I}, \boldsymbol{s} = \boldsymbol{0}, d = 0, \boldsymbol{t} = \boldsymbol{0}, s = 1\}$. These constraints are justified by the fact that the coarse model carries considerable physical characteristics of the fine model. Therefore, the optimum values of the mapping parameters should not severely deviate from the values corresponding to a unit mapping. To include these constraints, the objective function in (3) is modified as follows

$$\min_{\boldsymbol{c},\boldsymbol{B},\boldsymbol{s},d,\boldsymbol{t},s} \left\| \begin{bmatrix} \boldsymbol{e}_1^T & \boldsymbol{e}_2^T \cdots \boldsymbol{e}_N^T & \boldsymbol{c}^T & \boldsymbol{s}^T & \boldsymbol{t}^T & ?\boldsymbol{b}_1^T & ?\boldsymbol{b}_2^T \cdots ?\boldsymbol{b}_n^T & ?\ s & d \end{bmatrix}^T \right\| \tag{6}$$

where the error vectors $\boldsymbol{e}_1, \boldsymbol{e}_2, \cdots, \boldsymbol{e}_N$ are defined by (4a), the vectors $?\boldsymbol{b}_1, ?\boldsymbol{b}_2, \cdots, ?\boldsymbol{b}_n$ are the columns of the matrix $?\boldsymbol{B}$ given by

$$?\boldsymbol{B} = \boldsymbol{B} - \boldsymbol{I} \tag{7}$$

and $?s$ is defined by

$$\Delta s = s - 1 \tag{8}$$

The numerical values of the mapping parameters in (2) can give the designer physically-based intuitive information on the entire modeling process. The deviation of the optimal values of these parameters from those corresponding to a unit mapping indicates the degree of proximity between the coarse model and the fine model. This important feature can be used to compare between two coarse models. The coarse model with less deviation should be more accurate. Let β be the deviation of the mapping parameters from the parameters corresponding to a unit mapping, that is

$$\beta = \left\| [\boldsymbol{c}^T \ \boldsymbol{s}^T \ \boldsymbol{t}^T \ \Delta\boldsymbol{b}_1^T \ \Delta\boldsymbol{b}_2^T \cdots \Delta\boldsymbol{b}_n^T \ \Delta s \ \ d]^T \right\| \tag{9}$$

where $?\boldsymbol{b}_1, ?\boldsymbol{b}_2, \cdots, ?\boldsymbol{b}_n$ and $?s$ are defined by (7) and (8), respectively. Therefore, based on the value of β we can discriminate between various coarse models of the same device. The smaller the value of β the closer the coarse model is to the fine model. We will demonstrate this feature in one of the examples.

III. MULTIPLE SPACE MAPPING (MSM)

Multiple Space Mapping (MSM) was introduced in [3]. We present two variations of MSM for device modeling. We refer to them as MSM for Device Responses (MSMDR) and MSM for Frequency Intervals (MSMFI). In MSMDR we divide the device response vector $\boldsymbol{R}$ (in both models) into L subsets of responses (or vectors) $\boldsymbol{R}_i, i = 1, 2, ..., L$. An individual mapping is established for each subset of responses as illustrated in Fig. 4. In MSMFI we divide the frequency range of interest into M intervals and evaluate a separate mapping for each interval as illustrated in Fig. 5 (the switch in Fig. 5 is controlled by the frequency variable). The important questions are how we divide these responses into a set of sub-responses and how we divide the frequency range into a set of intervals. There was no guide in [3] regarding the answer to these questions. The following algorithms implement MSMDR and MSMFI.

MSMDR Algorithm

MSMDR algorithm divides the device responses in an iterative manner while establishing a separate mapping for each set of sub-responses. First it establishes a mapping targeting all responses. Then it assigns this mapping to the set of sub-responses satisfying a specified accuracy. It repeats the previous steps recursively on the remaining responses (which do not satisfy the required accuracy). The algorithm stops when all responses are exhausted. The following steps summarize the algorithm implementing MSMDR:

Step 1 Initialize i=1 and let $\boldsymbol{R}$ contain all responses.

Step 2 Establish a mapping $\boldsymbol{P}_i$, by solving (6), targeting all responses in $\boldsymbol{R}$.

Step 3 Assign the mapping $\boldsymbol{P}_i$ to the set of sub-responses $\boldsymbol{R}_i \subset \boldsymbol{R}$ that satisfies the error criteria $\left\| \boldsymbol{R}_{f_i} - \boldsymbol{R}_{c_i} \right\| \le e$, where e is a small positive number and $\boldsymbol{R}_{f_i}, \boldsymbol{R}_{c_i}$ are the fine and the coarse model sub-responses, respectively.

Step 4 Replace $\boldsymbol{R}$ by $\boldsymbol{R}_i - \boldsymbol{R}$ and increment i.

Step 5 If $\boldsymbol{R}$ is not empty go to step 2, otherwise stop.

We have to emphasize that MSMDR needs the same number of fine model simulations (EM simulations) required to establish a single mapping targeting all responses. However, it can dramatically improve the coarse models as we will see in the examples.

MSMFI Algorithm

MSMFI algorithm is similar to MSMDR algorithm. First it establishes a mapping targeting all set of responses $\boldsymbol{R}$ in the whole frequency range $\omega_{\min} \le \omega \le \omega_{\max}$. Then it assigns this mapping to the frequency interval $\omega_{\min} \le \omega \le \omega_1$ (where ω_1 belongs to the frequency range of interest) in which the set of responses $\boldsymbol{R}$ satisfies a certain specified accuracy. It repeats the previous steps recursively until covering the whole frequency range. The following steps summarize the MSMFI algorithm:

Step 1 Initialize i=1 and let the frequency interval $O = [?_{\min}, ?_{\max}]$.

Step 2 Establish a mapping $\boldsymbol{P}_i$, by solving (6), in the frequency range defined by O.

Step 3 Assign the mapping $\boldsymbol{P}_i$ to the frequency interval $O_i \subset O$ in which the error criteria $\left\| \boldsymbol{R}_f - \boldsymbol{R}_c \right\| \le e$ is satisfied, where e is a small positive number and $\boldsymbol{R}_f$, $\boldsymbol{R}_c$ are the fine and the coarse model responses, respectively.

Step 4 Replace O by $O - O_i$ and increment *i*.

Step 5 If O is not empty go to step 2, otherwise stop.

We have to emphasize that MSMFI costs the same number of fine model simulations (EM simulations) required to establish a single mapping for the whole frequency range.

IV. IMPLEMENTATION OF GSM

The optimization problem in (6) is solved using Huber optimizer [4] implemented in OSA90/hope [5]. The norm used in (6) is also a Huber norm [4]. Huber norm of an error vector $\boldsymbol{e} = [e_1\ e_2 \cdots e_l]^T$ is defined by [4]

$$H(\boldsymbol{e}) = \sum_{i=1}^{l} ?(e_i) \tag{10}$$

where

$$?(e_i) = \begin{cases} e_i^2 / 2 & \text{if} \quad |e_i| \le \alpha \\ \alpha\,|e_i| - \alpha^2 / 2 & \text{if} \quad |e_i| > \alpha \end{cases} \tag{11}$$

where α is a positive constant. The objective function in (6) is the Huber norm of the vector $\boldsymbol{e}$ given by

$$\boldsymbol{e} = [\ \boldsymbol{e}_1^T\ \boldsymbol{e}_2^T \cdots \boldsymbol{e}_N^T\ \boldsymbol{c}^T\ \boldsymbol{s}^T\ \boldsymbol{t}^T\ ?\,\boldsymbol{b}_1^T\ ?\,\boldsymbol{b}_2^T \cdots ?\,\boldsymbol{b}_n^T\ ?\ s\ d]^T \tag{12}$$

The Huber norm is robust against large errors and flexible with respect to small variations in the data [4]. The set of base points $\{\boldsymbol{x}_{f_i}, i = 1, 2, ..., B_p\}$ in the region of interest is taken as in [6] (see Fig. 6). According to this distribution the number of base points is 2*n*+1 where *n* is the number of fine model parameters. The starting values for the mapping parameters $\{\boldsymbol{c}, \boldsymbol{B}, \boldsymbol{s}, d, \boldsymbol{t}, s\}$ are $\{\boldsymbol{0}, \boldsymbol{I}, \boldsymbol{0}, 0, \boldsymbol{0}, 1\}$ which correspond to the unit mapping $\boldsymbol{x}_c = \boldsymbol{x}_f$ and $?_c = ?$. The software tools needed for the implementation

of GSM are an optimizer (Huber optimizer [4] is recommended), a suitable circuit simulator which can handle simple matrix operations, and a suitable full-wave EM simulator.

V. EXAMPLES

We present four typical modeling problems: a microstrip line, a microstrip right angle bend, a microstrip step junction and a microstrip shaped T-junction. To display the results in a compact way we define the error E_{ij} as the modulus of the difference between the scattering parameter S_{ij}^f computed by the fine model and the scattering parameter S_{ij}^c computed by the coarse model

$$E_{ij} = \left| S_{ij}^f - S_{ij}^c \right| = \sqrt{(\mathrm{Re}[S_{ij}^f] - \mathrm{Re}[S_{ij}^c])^2 + (\mathrm{Im}[S_{ij}^f] - \mathrm{Im}[S_{ij}^c])^2} \tag{13}$$

where i=1,2,..., M and j=1, 2,..., M (M is the number of ports of the microwave device). The error E_{ij} is a measure of both the error in the magnitude and the phase of the scattering parameters S_{ij}^c. We refer to E_{ij} simply as the error in the scattering parameter S_{ij}.

Microstrip Line

In this example we compare between SMSM and FSMSM. Both modeling approaches are used to enhance the transmission line model of a microstrip line. The fine model is analyzed by Sonnet's ***em*** simulator [7] and the "coarse" model is a built-in element of OSA90/hope [5]. The fine and coarse models are shown in Fig 7. The structure in Fig. 7(a) was parameterized using Geometry Capture [8] implemented in Empipe^{TM} [9]. The fine and coarse model parameters are given by $\boldsymbol{x}_f = [L\ W\ H\ \varepsilon_r]^T$, $\boldsymbol{x}_c = [L_c\ W_c\ H_c\ \varepsilon_{rc}]^T$. The region of interest is given in Table I. The frequency range is 20 GHz to 30 GHz with a step of 2 GHz (F_p = 6). The characteristic impedance Z_0 of the transmission line is computed in terms of the width W_c, the substrate height H_c and the relative dielectric constant ε_{rc} using the quasi-static model in [10]. Only 9 points (B_p = 9) in the region of interest were used to develop SMSM or FSMSM. We developed SMSM and FSMSM for the microstrip line and the corresponding mapping parameters for each case are given in Table II. Notice that in case of SMSM the mapping parameters $\boldsymbol{s}, d, \boldsymbol{t}, s$ are fixed and in the case of FSMSM the computed value of $\boldsymbol{t}$ is $\mathbf{0}$ which means that the coarse

model frequency does not depend on the fine model parameters (it only depends on the fine model frequency). The microstrip transmission line SMSM and FSMSM were tested at 50 uniformly distributed random points in the region of interest. The error in S_{21} defined by (13) for the microstrip transmission line model is shown in Fig. 8(a). Figs. 8(b) and (c) show the error in S_{21} by the microstrip transmission line SMSM and by the microstrip transmission line FSMSM, respectively. The error of the microstrip transmission line FSMSM is approximately 4 times less than the corresponding error of the microstrip transmission line SMSM.

Microstrip Right Angle Bend

In this example we compare between two coarse models for the microstrip right angle bend. The first coarse model is taken from [11] and is referred to as Gupta's model. The second coarse model is taken from [12] and is referred to as Jansen's model. Both coarse models provide empirical formulas for the LC circuit in Fig. 9. The fine model is analyzed by Sonnet's ***em*** [7] as shown in Fig. 9 (a). The fine and coarse model parameters are given by $\boldsymbol{x}_f = [W\ H\ \varepsilon_r]^T$, $\boldsymbol{x}_c = [W_c\ H_c\ \varepsilon_{rc}]^T$. The region of interest is given in Table III. The frequency range is 1 GHz to 31 GHz with a step of 2 GHz ($F_p = 16$). The number of base points in the region of interest is 7 ($B_p = 7$).

The FSMSM was developed for the two coarse models and the corresponding mapping parameters are given in Table IV. The enhanced Gupta's model and the enhanced Jansen's model were tested at 50 random points in the region of interest. The error in S_{11} by the Gupta's model and by the Jansen's model is shown in Fig. 10. The error in S_{11} by the enhanced Gupta's model and by the enhanced Jansen's model is shown in Fig. 11.

It is difficult to compare between the two coarse models since Jansen's model is more accurate at lower frequencies (see Fig. 10) and Gupta's model is slightly more accurate at higher frequencies. However, after developing FSMSM for each coarse model we can compare between the two coarse models according to the criteria in Section II. The values of β given by (9) for the enhanced Gupta's model and for the enhanced Jansen's model are 3.4 and 3.5, respectively. We notice that the value of β

in both cases is approximately the same, which means that the accuracy of both coarse models with respect to the fine model is comparable.

Microstrip Step Junction

In this example we demonstrate the MSMDR. The fine model of the microstrip step junction (Fig. 12) is analyzed by Sonnet's ***em*** [4]. The "coarse" model is a built-in element of OSA90/hope [6]. The fine and coarse model parameters are given by $\boldsymbol{x}_f = [W_1\ W_2\ H\ \varepsilon_r]^T$, $\boldsymbol{x}_c = [W_{1c}\ W_{2c}\ H_c\ \varepsilon_{rc}]^T$. The region of interest is given in Table V. The frequency range is 2 GHz to 40 GHz with a step of 2 GHz (F_p = 20). The number of base points in the region of interest is 9 (B_p = 9). There are six responses to be matched: the real and imaginary parts of S_{11}, S_{21} and S_{22}. We will show that one mapping targeting all these responses is not sufficient to achieve the required accuracy at the base points. The required accuracy is $E_{ij} \le 0.03,\ i = 1, 2$ and $j = 1, 2$ where E_{ij} is defined by (13). Fig. 13(a) shows the error in S_{11} before applying any modeling technique while Fig. 13(b) shows it after developing a single mapping for all responses. The results obtained by a single mapping do not satisfy the required accuracy.

The MSMDR algorithm (in Section III) was applied to align the two models. The algorithm divided the responses into two groups {Im[S_{11}], Im[S_{21}], Im[S_{22}], Re[S_{21}])} and {Re[S_{11}], Re[S_{22}]} and developed a separate mapping for each group of responses. The corresponding mapping parameters for each group are given in Table VI. Fig. 13(c) shows the error in S_{11} at the base points after applying the MSMDR algorithm. We notice that the specified accuracy is achieved.

The enhanced coarse model of the step junction was tested at 50 uniformly distributed random points. The errors in S_{11} and S_{21} by the coarse model are shown in Figs. 14(a) and (b), respectively. The errors in S_{11} and S_{21} by the enhanced coarse model are shown in Figs. 15(a) and (b), respectively. The histograms of the error in S_{21} at 40 GHz (which is the maximum error in the frequency range 2GHz to 40 GHz) by the coarse model and by the enhanced coarse model are shown in Figs. 16(a) and (b), respectively. The mean and standard deviation for the two cases are also shown in Figs. 16(a) and (b).

Microstrip Shaped T-Junction

In this example we consider a shaped T-junction (Fig. 17(a)). This T-junction was introduced in [13] to compensate discontinuities. It was recently compared in [14] with the other T-junction configurations in the literature. The T-junction is symmetric in the sense that all input lines have the same width w. The fine model is analyzed by Sonnet's ***em*** [7] and the coarse models is composed of empirical models of simple microstrip elements (see Fig. 17(b)) of OSA90/hope [5]. The fine and coarse model parameters are given by $\boldsymbol{x}_f = [\, w \;\; h \;\; w_1 \; w_2 \; x \; y \;\; e_r \,]^T$, $\boldsymbol{x}_c = [\, w_c \;\; h_c \; w_{1c} \; w_{2c} \; x_c \; y_c \;\; e_{cr} \,]^T$.

The region of interest is given in Table VII and the frequency range used is 2 GHz to 20 GHz with a step of 2 GHz (F_p = 10). The width w of the input lines is determined in terms of h and e_r so that the characteristic impedance of the input lines is 50 ohm. The width w_1 is taken as 1/3 of the width w. The width w_2 is obtained so that the characteristic impedance of the microstrip line after the step connected to port 2 is twice the characteristic impedance of the microstrip line after the step connected to port 1 (see Fig. 17(b)). The number of base points in the region of interest is 9 (B_p = 9).

The MSMFI algorithm (in Section III) was applied to enhance the accuracy of the T-Junction coarse model. The algorithm divided the total frequency range into two intervals: 2 GHz to 16 GHz and 16 GHz to 20 GHz. The corresponding mapping parameters for each interval are given in Table VIII. Figs. 18(a) and (b) show $|S_{11}|$ and $|S_{22}|$ by Sonnet's ***em*** [7], the T-junction coarse model and the T-junction enhanced coarse model at two test points in the region of interest. To perform a more comprehensive test, 50 random points were generated in the region of interest. The coarse model errors in S_{11} and in S_{22} defined by (13) are shown in Figs. 19(a) and (b), respectively. The enhanced coarse model errors in S_{11} and in S_{22} are shown in Figs. 20(a) and (b), respectively.

The enhanced coarse model for the shaped T–Junction can be utilized in optimization. For example, the T-junction is optimized here to achieve the possible minimum mismatch at the three ports. The optimization variables are x and y, the other parameters are kept fixed (w = 24 mil, h = 25 mil and $\varepsilon_r = 9.9$) [14]. The specifications [14] are $|S_{11}| \le 1/3$, $|S_{22}| \le 1/3$ in the frequency range 2 GHz to 16

GHz. The minimax optimizer in OSA90/hope [5] reached the solution x = 2.1 mil and y = 21.1 mil, which agrees with the solution obtained in [14]. The magnitude of S_{11} and S_{22} obtained by Sonnet's ***em*** [7], the coarse model and the enhanced coarse model are shown in Figs. 21(a) and (b). We notice a good agreement between the results obtained by the enhanced coarse model and by Sonnet's ***em***.

VI. CONCLUSIONS

The powerful GSM approach to device modeling is introduced. Three derivative concepts are illustrated: the SMSM concept, the FSMSM concept and the MSM concept. Two variations of MSM are also presented: MSMDR and MSMFI. Our approach typically uses only a few EM simulations to dramatically enhance the accuracy of existing empirical device models. It involves only simple matrix operations which makes it an effective CAD tool in terms of CPU time, memory requirement, ease of use and accuracy. It also preserves the compactness and simplicity of the original empirical models. Three software tools are required to implement GSM: an optimizer (Huber optimizer is recommended since it is robust against large errors in the data), a suitable circuit simulator and a suitable full-wave EM simulator.

ACKNOWLEDGEMENT

The authors would like to thank Dr. R.M. Biernacki and Dr. S.H. Chen, former colleagues both now with HP EEsof, Santa Rosa, CA, for useful discussions on the Space Mapping Super Model concept at an early stage of its development. The authors also thank Dr. J.C. Rautio, President, Sonnet Software, Inc., Liverpool, NY, for making ***em***™ available.

REFERENCES

[1] J.W. Bandler, R.M. Biernacki, S.H. Chen, P.A. Grobelny and R.H. Hemmers, "Space mapping technique for electromagnetic optimization," *IEEE Trans. Microwave Theory Tech.*, vol. 42, 1994, pp. 2536-2544.

[2] J.W. Bandler, R.M. Biernacki, S.H. Chen, R.H. Hemmers and K. Madsen, "Electromagnetic optimization exploiting aggressive space mapping," *IEEE Trans. Microwave Theory Tech.*, vol. 43, 1995, pp. 2874-2882.

[3] J.W. Bandler, R.M. Biernacki, S.H. Chen and Q.H. Wang, "Multiple space mapping EM optimization of signal integrity in high-speed digital circuits," *Proc. 5th Int. Workshop on Integrated Nonlinear Microwave and Millimeterwave Circuits* (Duisburg, Germany), 1998, pp. 138-140.

[4] J.W. Bandler, S.H. Chen, R.M. Biernacki, L. Gao, K. Madsen and H. Yu, "Huber optimization of circuits: a robust approach," *IEEE Trans. Microwave Theory Tech.*, vol. 41, 1993, pp. 2279-2287.

[5] *OSA90/hope*™ Version 4.0, formerly Optimization Systems Associates Inc., P.O. Box 8083, Dundas, Ontario, Canada L9H 5E7, now HP EEsof Division, Hewlett-Packard Company, 1400 Fountaingrove, Parkway, Santa Rosa, CA 95403-1799.

[6] R.M. Biernacki, J.W. Bandler, J. Song and Q.J. Zhang, "Efficient quadratic approximation for statistical design," *IEEE Trans. Circuit Syst.*, vol. 36, 1989, pp. 1449-1454.

[7] ***em***™ Version 4.0b, Sonnet Software, Inc., 1020 Seventh North Street, Suite 210, Liverpool, NY 13088, 1997.

[8] J.W. Bandler, R.M. Biernacki and S.H. Chen, "Parameterization of arbitrary geometrical structures for automated electromagnetic optimization," *IEEE MTT-S Int. Microwave Symp. Dig.* (San Francisco, CA), 1996, pp. 1059-1062.

[9] *Empipe*™ Version 4.0, formerly Optimization Systems Associates Inc., P.O. Box 8083, Dundas, Ontario, Canada L9H 5E7, now HP EEsof Division, Hewlett-Packard Company, 1400 Fountaingrove, Parkway, Santa Rosa, CA 95403-1799.

[10] D.M. Pozar, *Microwave Engineering*. New York: Addison-Wesley, 1990.

[11] K.C. Gupta, R. Garg, I.J. Bahl, *Microstrip Lines and Slotlines*. Dedham, MA: Artech House, 1979.

[12] M. Kirschning, R. Jansen and N. Koster, "Measurement and computer-aided modeling of microstrip discontinuities by an improved resonator method," *IEEE MTT-S Int. Microwave Symp. Dig.* (Boston, MA), 1983, pp. 495-497.

[13] M. Dydyk, "Master the T-junction and sharpen your MIC designs," *Microwaves*, 1977, pp. 184-186.

[14] J.W. Bandler, M.H. Bakr, N. Georgieva, M.A. Ismail and D.G. Swanson, Jr., "Recent results in electromagnetic optimization of microwave components including microstrip T-junctions," *Applied Computational Electromagnetics Society Conf.* (Monterey, CA), 1999, pp. 326-333.

TABLE I
REGION OF INTEREST FOR THE
MICROSTRIP LINE EXAMPLE

Parameter	Minimum value	Maximum value
W	10 mil	30 mil
L	40 mil	60 mil
H	10 mil	20 mil
ε_r	8	10

TABLE II
THE SMSM AND FSMSM MAPPING PARAMETERS
FOR THE MICROSTRIP TRANSMISSION LINE

	SMSM	FSMSM
$\boldsymbol{B}$	$\begin{bmatrix} 1.015 & -0.002 & -0.007 & -0.022 \\ -0.001 & 0.992 & 0.020 & 0.023 \\ -0.008 & 0.001 & 0.985 & 0.027 \\ 0.009 & -0.004 & 0.044 & 1.028 \end{bmatrix}$	$\begin{bmatrix} 1.026 & -0.005 & 0.006 & -0.021 \\ -0.009 & 0.965 & -0.011 & 0.017 \\ -0.002 & 0.004 & 0.979 & 0.022 \\ 0.019 & -0.001 & 0.020 & 1.025 \end{bmatrix}$
$\boldsymbol{c}$	$[-0.011 \quad -0.008 \quad 0.012 \quad -0.036]^T$	$[-0.013 \quad 0.001 \quad 0.011 \quad -0.010]^T$
$\boldsymbol{s}$	$\mathbf{0}$ (fixed)	$[-0.006 \quad 0 \quad 0.002 \quad -0.002]^T$
$\boldsymbol{t}$	$\mathbf{0}$ (fixed)	$\mathbf{0}$
s	1 (fixed)	1.035
d	0 (fixed)	0.001

TABLE III
REGION OF INTEREST FOR THE
MICROSTRIP RIGHT ANGLE BEND

Parameter	Minimum value	Maximum value
W	20 mil	30 mil
H	8 mil	16 mil
ε_r	8	10

TABLE IV
THE FSMSM MAPPING PARAMETERS FOR
THE MICROSTRIP RIGHT ANGLE BEND

	Gupta's model [11]	Jansen's model [12]
$\boldsymbol{B}$	$\begin{bmatrix} 1.291 & 0.207 & 0.189 \\ 0.067 & 0.613 & -0.094 \\ 0.092 & -0.066 & 0.918 \end{bmatrix}$	$\begin{bmatrix} 2.768 & 0.314 & 0.276 \\ -0.042 & 1.282 & 0.318 \\ -0.018 & -0.013 & 0.421 \end{bmatrix}$
$\boldsymbol{c}$	$[0.094 \quad -0.174 \quad 0.123]^T$	$[0.048 \quad -0.012 \quad 0.031]^T$
$\boldsymbol{s}$	$[0.109 \quad -0.296 \quad 0.183]^T$	$[0.001 \quad -0.053 \quad 0.250]^T$
$\boldsymbol{t}$	$[-0.001 \quad -0.002 \quad -0.002]^T$	$[-0.001 \quad -0.002 \quad -0.001]^T$
s	3.269	2.343
d	0.019	0.015

TABLE V
REGION OF INTEREST FOR THE
MICROSTRIP STEP JUNCTION

Parameter	Minimum value	Maximum value
W_1	20 mil	40 mil
W_2	10 mil	20 mil
H	10 mil	20 mil
ε_r	8	10

TABLE VI
THE MSMDR MAPPING PARAMETERS FOR THE
MICROSTRIP STEP JUNCTION

	Target responses are $\{\mathrm{Im}[S_{11}], \mathrm{Im}[S_{21}], \mathrm{Im}[S_{22}], \mathrm{Re}[S_{21}])\}$	Target responses are $\{\mathrm{Re}[S_{11}], \mathrm{Re}[S_{22}]\}$
$\boldsymbol{B}$	$\begin{bmatrix} 0.764 & 0.033 & -0.062 & 0.074 \\ 0.191 & 0.632 & 0.255 & -0.502 \\ -0.023 & 0.116 & 1.485 & 0.018 \\ 0.676 & -0.365 & -0.111 & 0.177 \end{bmatrix}$	$\begin{bmatrix} 3.071 & -0.008 & -0.010 & -0.004 \\ 0.008 & 0.202 & 0.032 & 0.004 \\ -0.001 & 0.001 & 1.152 & 0.000 \\ -0.077 & -0.118 & -0.002 & 1.241 \end{bmatrix}$
$\boldsymbol{c}$	$[0.002 \quad -0.002 \quad 0.002 \quad -0.006]^T$	$[-0.001 \quad 0.001 \quad 0.000 \quad -0.003]^T$
$\boldsymbol{s}$	$[-0.003 \quad 0.004 \quad -0.001 \quad -0.002]^T$	$\mathbf{0}$
$\boldsymbol{t}$	$[-0.001 \quad 0.000 \quad -0.005 \quad 0.000]^T$	$[-0.001 \quad 0.000 \quad -0.007 \quad 0.003]^T$
s	1.546	5.729
d	0.113	0.065

TABLE VII
REGION OF INTEREST FOR THE
MICROSTRIP SHAPED T-JUNCTION

Parameter	Minimum value	Maximum value
h	15 mil	25 mil
x	5 mil	15 mil
y	5 mil	15 mil
ε_r	8	10

TABLE VIII
THE MSMFI MAPPING PARAMETERS
FOR THE MICROSTRIP SHAPED T-JUNCTION

	2 GHz to 16 GHz	16 GHz to 20 GHz
$\boldsymbol{B}$	$\begin{bmatrix} 1.04 & 0.07 & 0.01 & 0.08 & -0.06 & 0.00 & 0.22 \\ 0.00 & 0.89 & 0.00 & -0.07 & -0.20 & 0.06 & -0.03 \\ -0.00 & 0.07 & 0.99 & 0.04 & -0.12 & 0.01 & -0.06 \\ -0.04 & 0.00 & -0.01 & 0.97 & 0.10 & -0.06 & -0.27 \\ 0.01 & 0.04 & 0.00 & 0.03 & 0.99 & -0.05 & -0.03 \\ -0.13 & -0.05 & -0.04 & -0.16 & 0.12 & 0.99 & 0.62 \\ -0.08 & 0.12 & -0.03 & 0.00 & -0.07 & 0.03 & 0.83 \end{bmatrix}$	$\begin{bmatrix} 0.99 & 0.02 & -0.00 & 0.01 & -0.09 & -0.01 & 0.13 \\ 0.05 & 0.85 & 0.01 & -0.07 & -0.28 & 0.01 & -0.01 \\ -0.06 & 0.15 & 0.98 & 0.04 & -0.25 & 0.00 & 0.02 \\ -0.10 & -0.06 & -0.03 & 0.88 & 0.13 & -0.09 & -0.27 \\ 0.08 & 0.04 & 0.03 & 0.11 & 1.07 & -0.04 & -0.12 \\ -0.14 & -0.02 & -0.05 & -0.15 & 0.23 & 1.03 & 0.51 \\ -0.13 & 0.22 & -0.04 & 0.02 & -0.07 & 0.03 & 0.87 \end{bmatrix}$
$\boldsymbol{c}$	$[\,0.02 \quad 0.01 \quad -0.01 \quad -0.03 \quad -0.01 \quad 0.07 \quad -0.03\,]^T$	$[\,0.01 \quad 0.01 \quad -0.01 \quad -0.03 \quad -0.01 \quad 0.05 \quad -0.03]^T$
$\boldsymbol{s}$	$[-0.01 \quad 0.09 \quad -0.10 \quad -0.02 \quad 0.00 \quad -0.02 \quad -0.20\,]^T$	$[\,0.00 \quad 0.01 \quad -0.01 \quad 0.00 \quad 0.00 \quad 0.00 \quad -0.02]^T$
$\boldsymbol{t}$	$\mathbf{0}$	$[\,0.01 \quad 0.00 \quad -0.02 \quad 0.00 \quad 0.00 \quad 0.00 \quad 0.00]^T$
s	0.851	0.957
d	–0.003	0.008

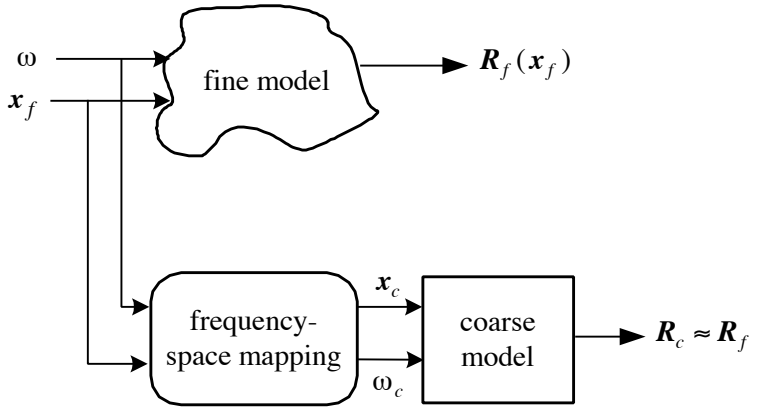

Fig. 1. The Frequency-Space Mapping Super Model (FSMSM) concept.

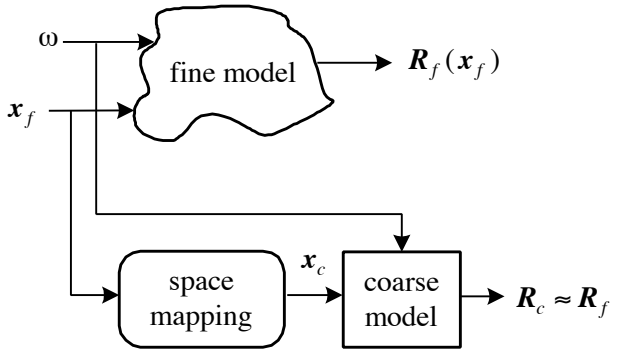

Fig. 2. The Space Mapping Super Model (SMSM) concept.

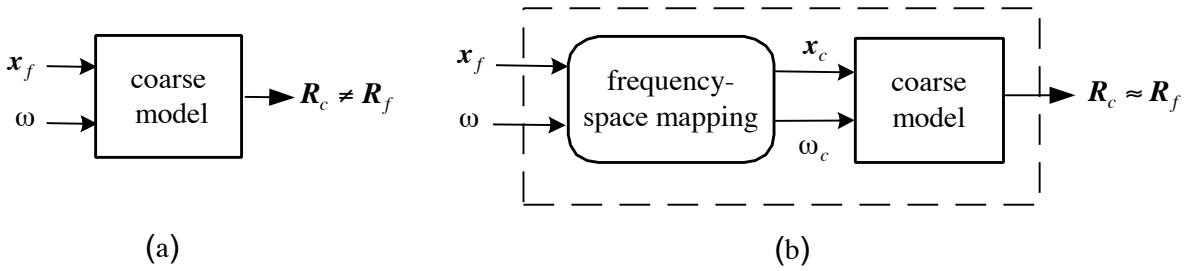

Fig. 3. The coarse model (a) and the enhanced coarse model (b).

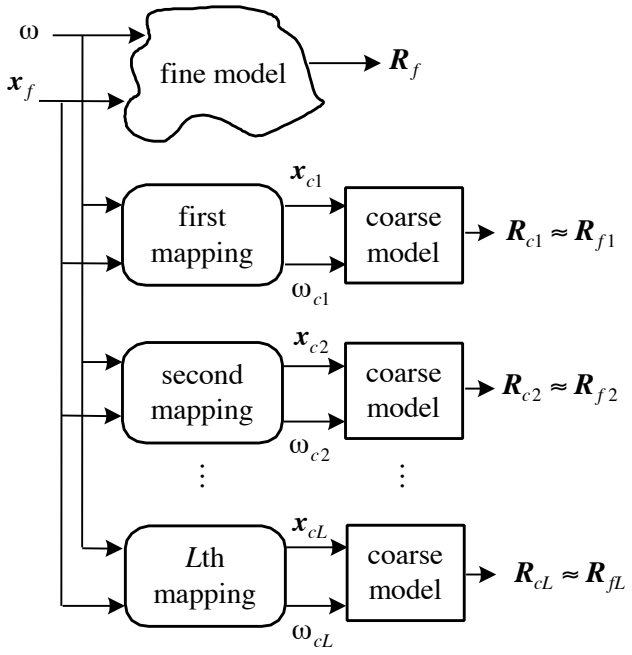

Fig. 4. The Multiple Space Mapping for Device Responses (MSMDR).

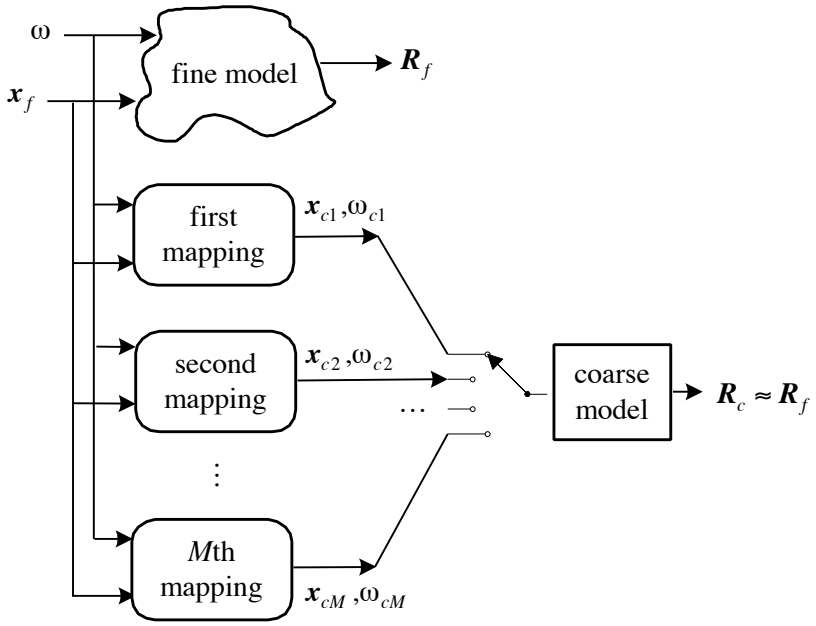

Fig. 5. The Multiple Space Mapping for Frequency Intervals (MSMFI).

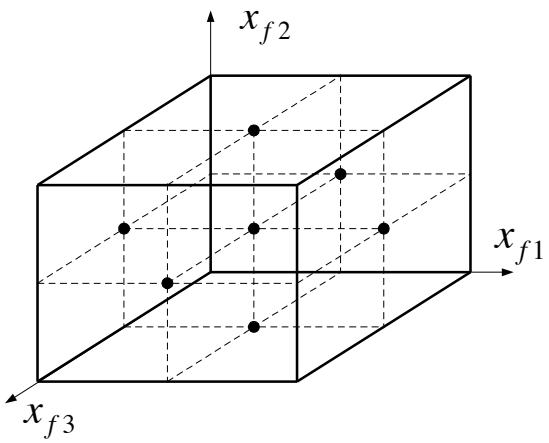

Fig. 6. Distribution of the base points in the region of interest for a 3-dimensional space [6].

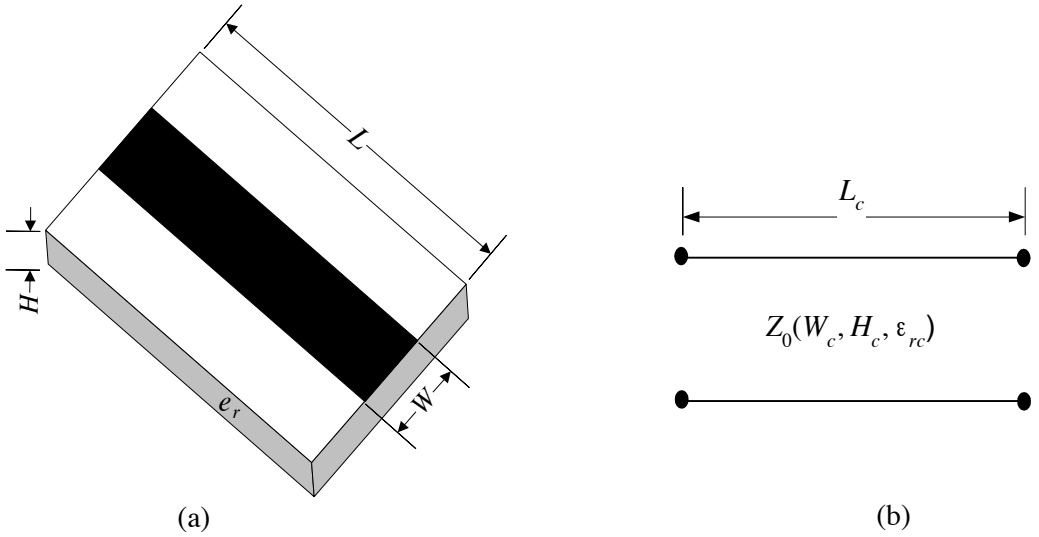

Fig. 7. Microstrip line models: (a) the fine model; (b) the coarse model.

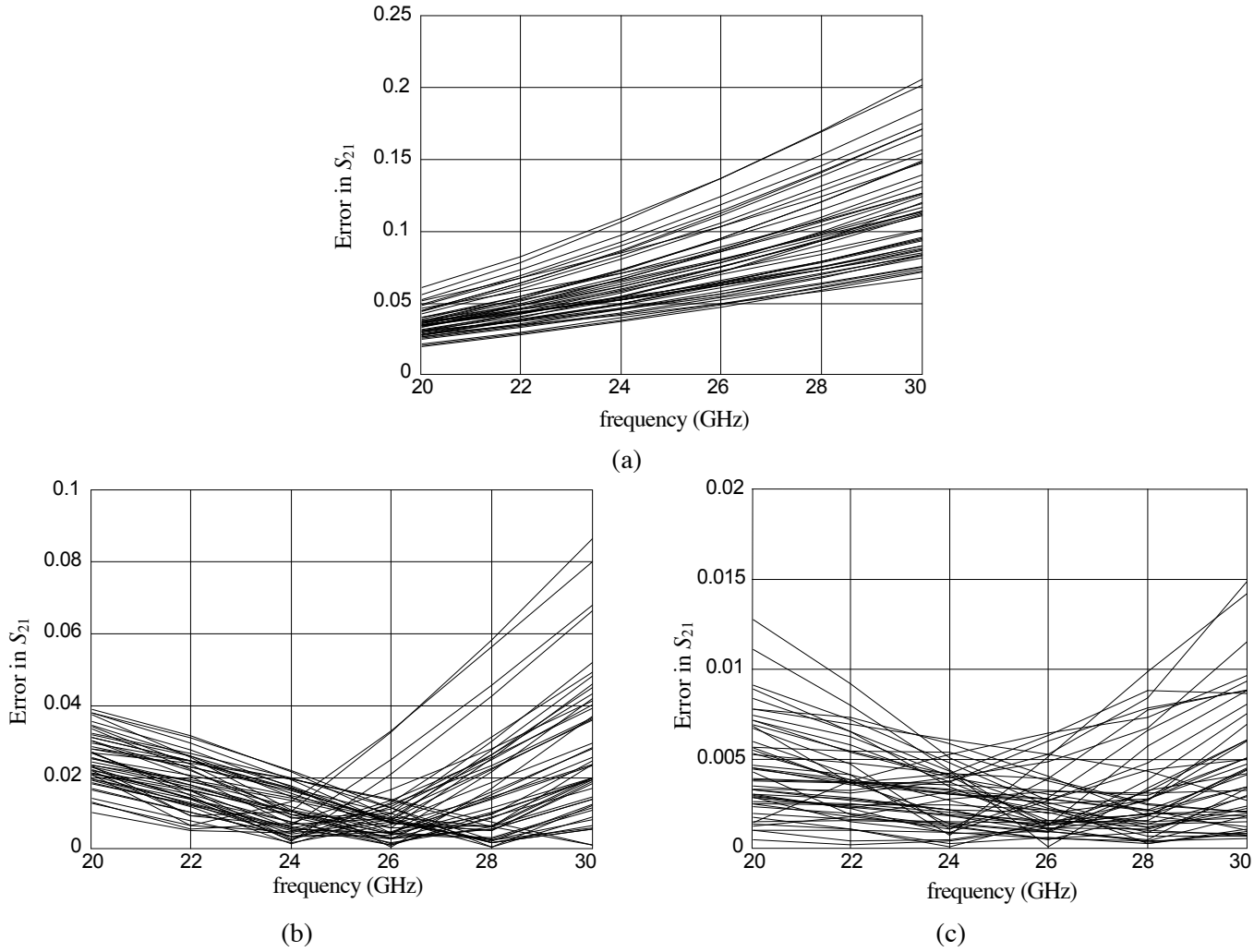

Fig. 8. Error in S_{21} with respect to ***em***™: (a) by the microstrip transmission line model; (b) by the microstrip transmission line SMSM; (c) by the microstrip transmission line FSMSM.

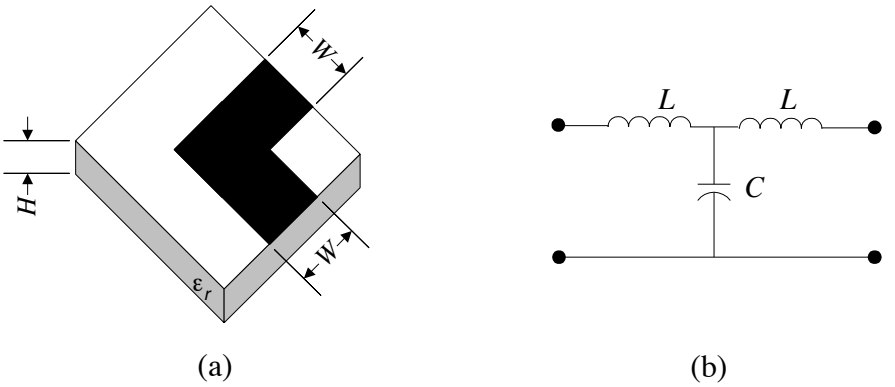

Fig. 9. Microstrip right angle bend: (a) the fine model; (b) the coarse model.

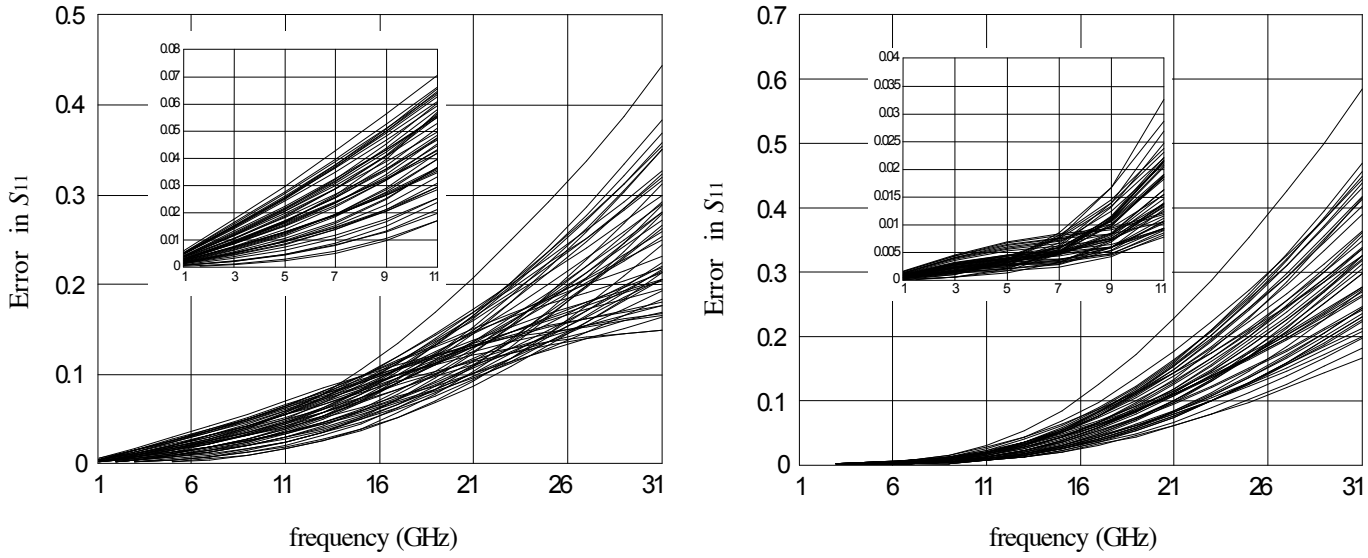

Fig. 10. Error in S_{11} of the microstrip right angle bend with respect to ***em***™: (a) by Gupta's model [11]; (b) by Jansen's model [12].

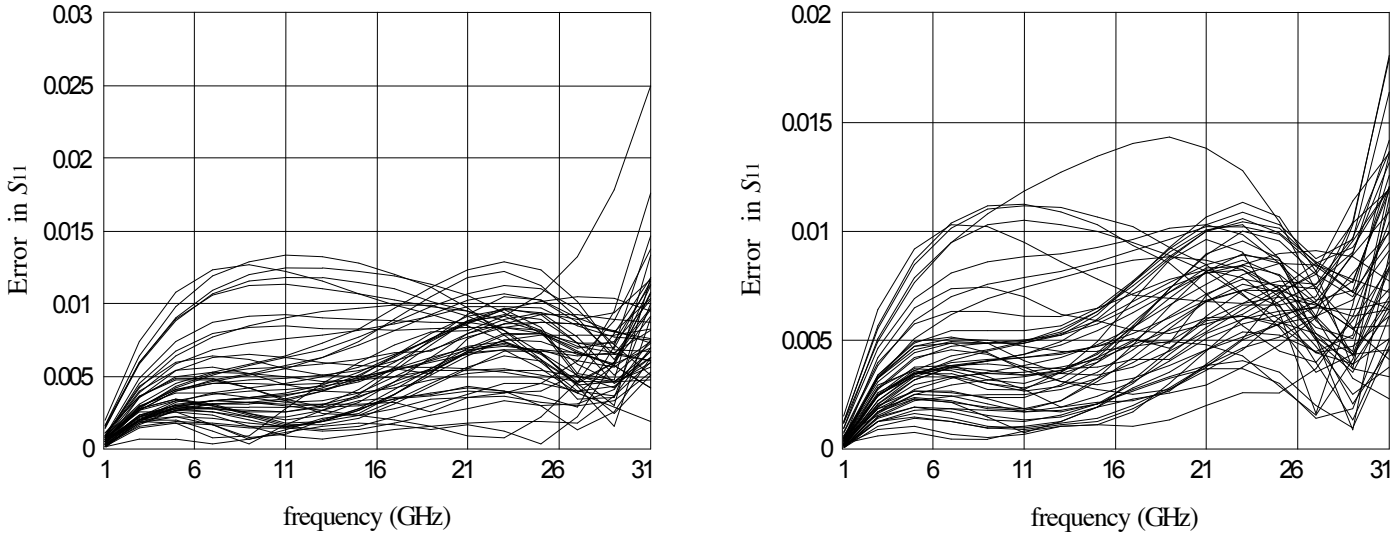

Fig. 11. Error in S_{11} of the microstrip right angle bend with respect to ***em***™: (a) by the enhanced Gupta's model [11]; (b) by the enhanced Jansen's model [12].

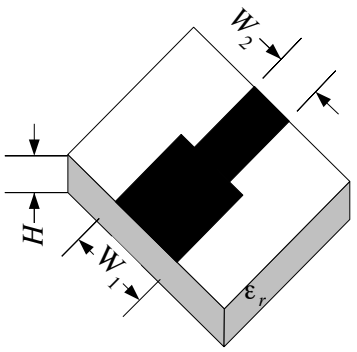

Fig. 12. Microstrip step junction.

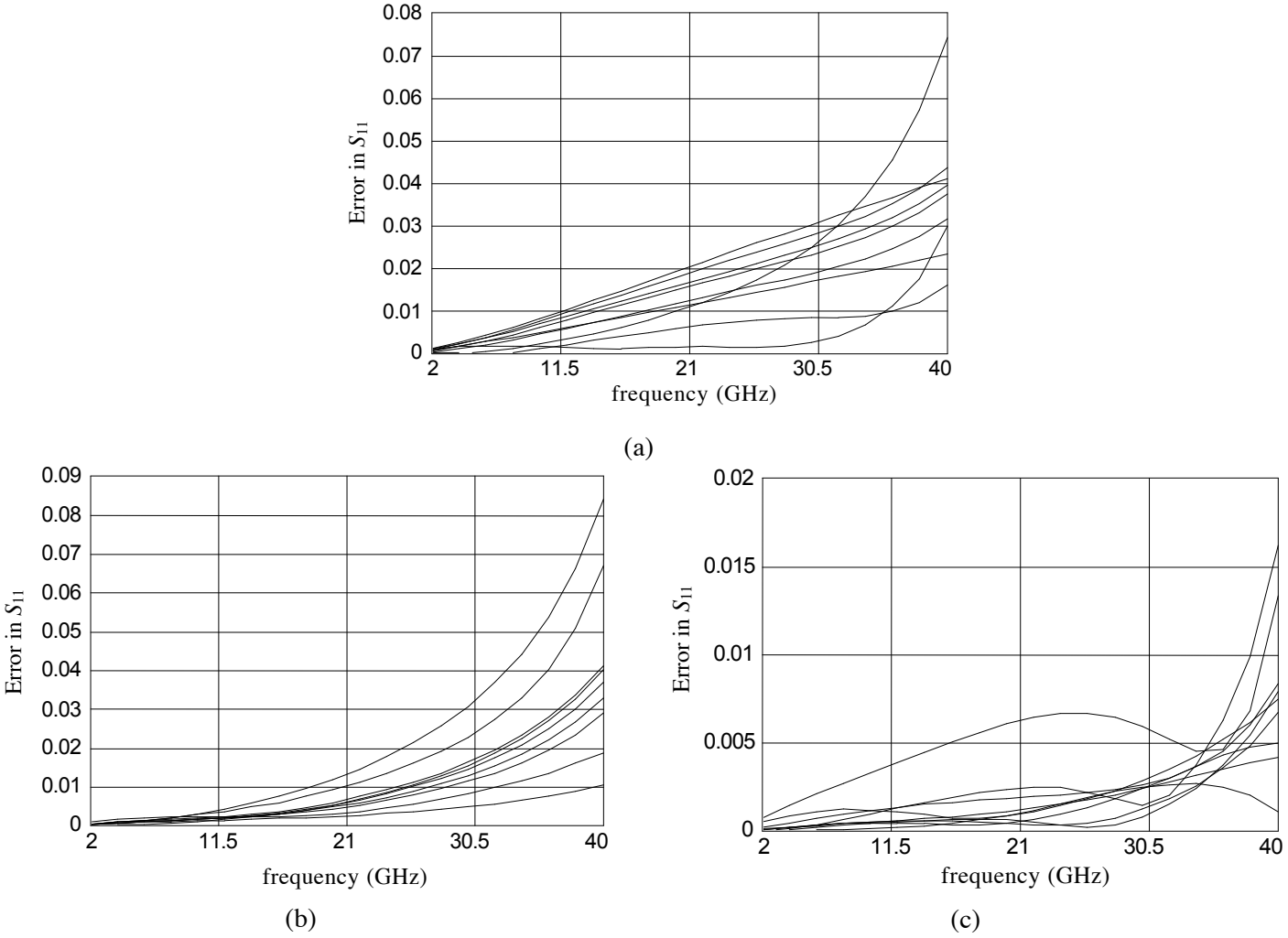

Fig. 13. Error in S_{11} of the microstrip step junction with respect to ***em***™: (a) before applying any modeling technique; (b) after applying FSMSM; (c) after applying the MSMDR algorithm.

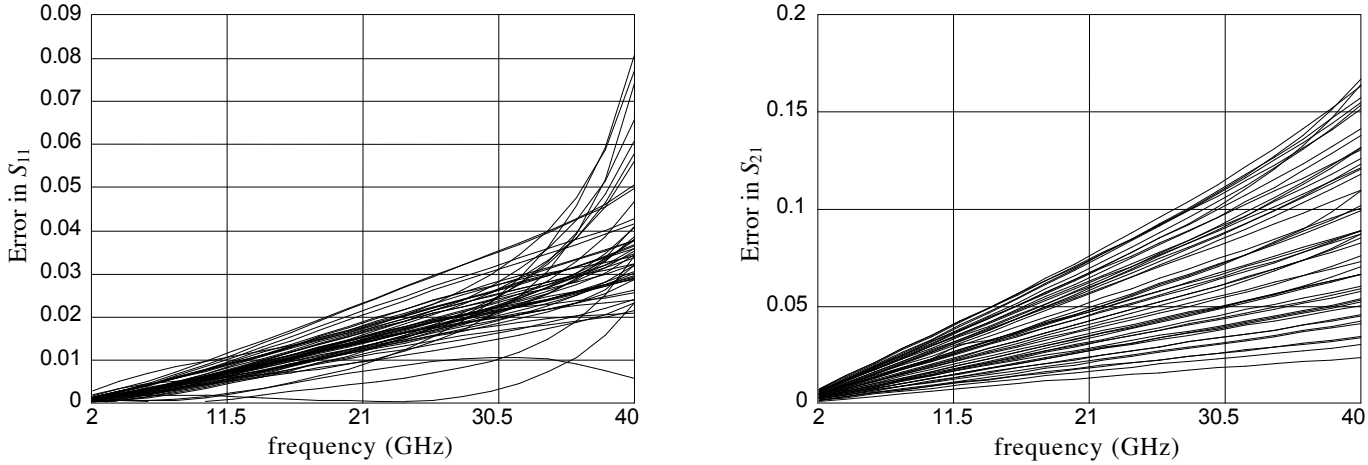

Fig. 14. Error of the microstrip step junction coarse model with respect to ***em***™: (a) in S_{11}; (b) in S_{21}.

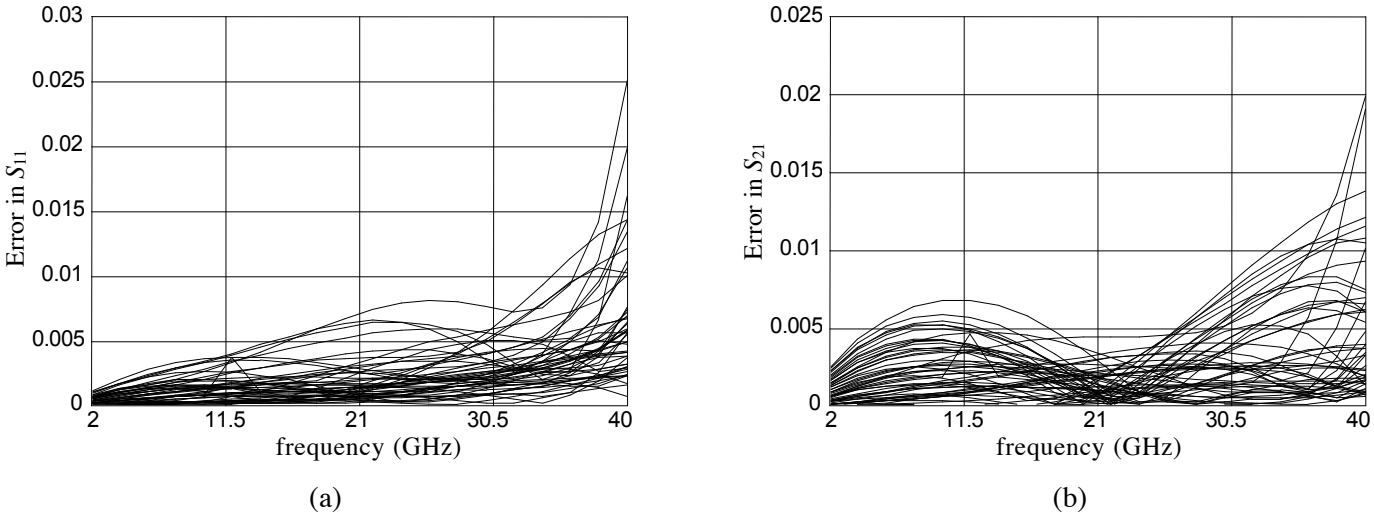

Fig. 15. Error of the microstrip step junction enhanced coarse model with respect to ***em***™: (a) in S_{11}; (b) in S_{21}.

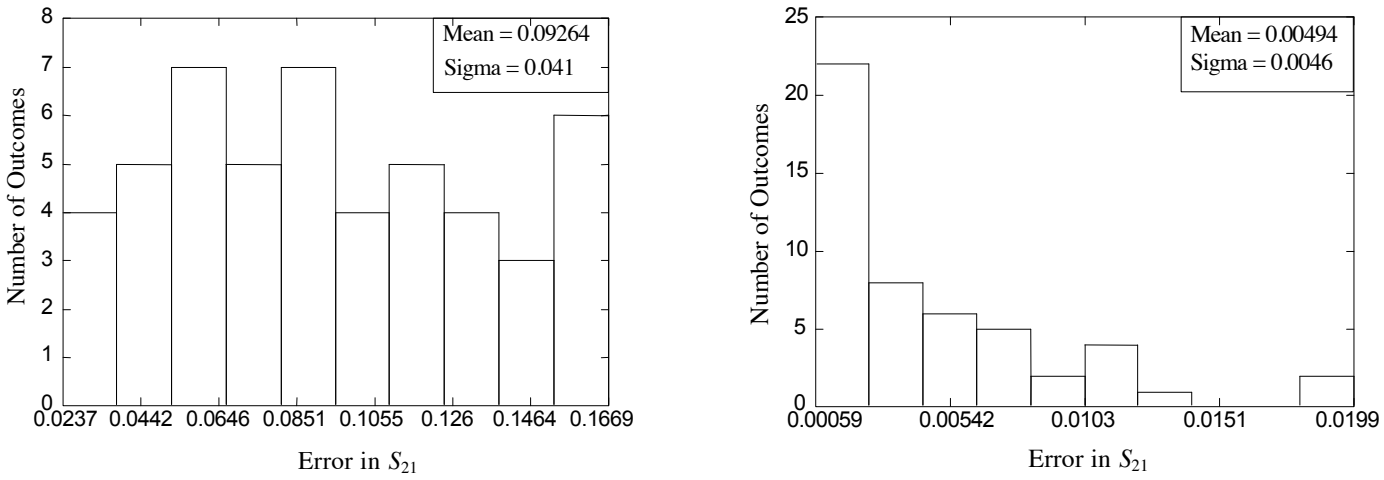

Fig. 16. Histogram of the error in S_{21} of the microstrip step junction for 50 points in the region of interest at 40 GHz: (a) by the coarse model; (b) by the enhanced coarse model.

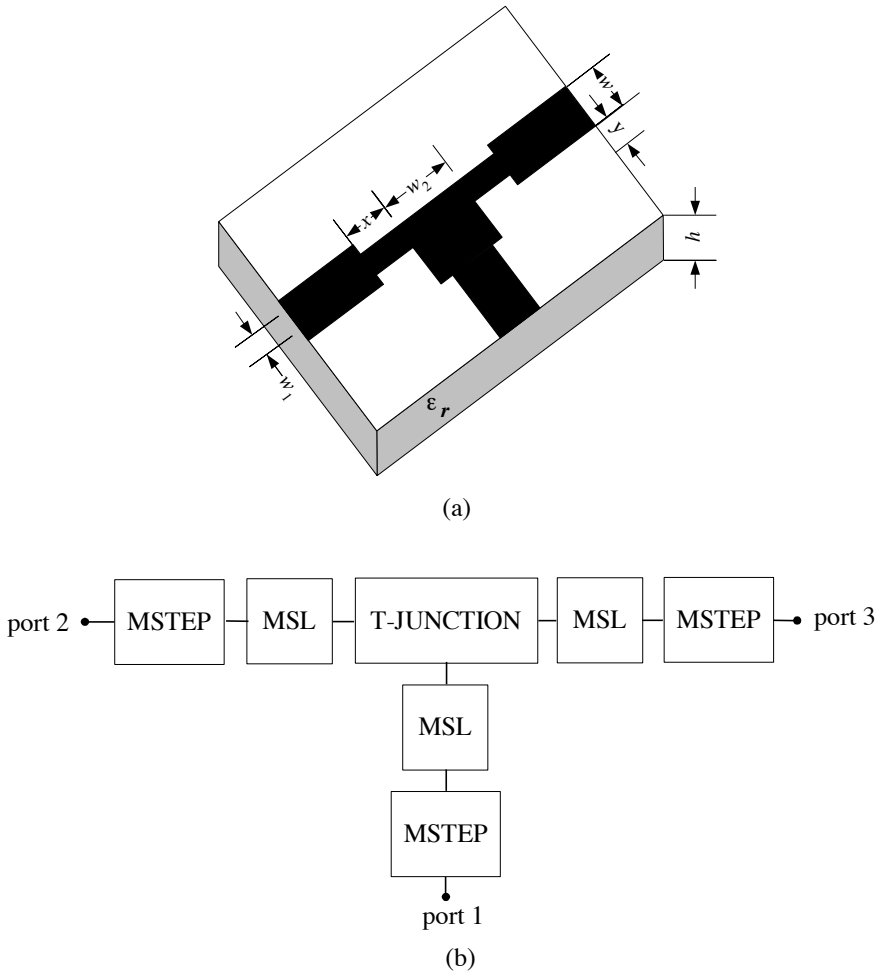

Fig. 17. Microstrip shaped T-junction: (a) the physical structure (fine model); (b) the coarse model.

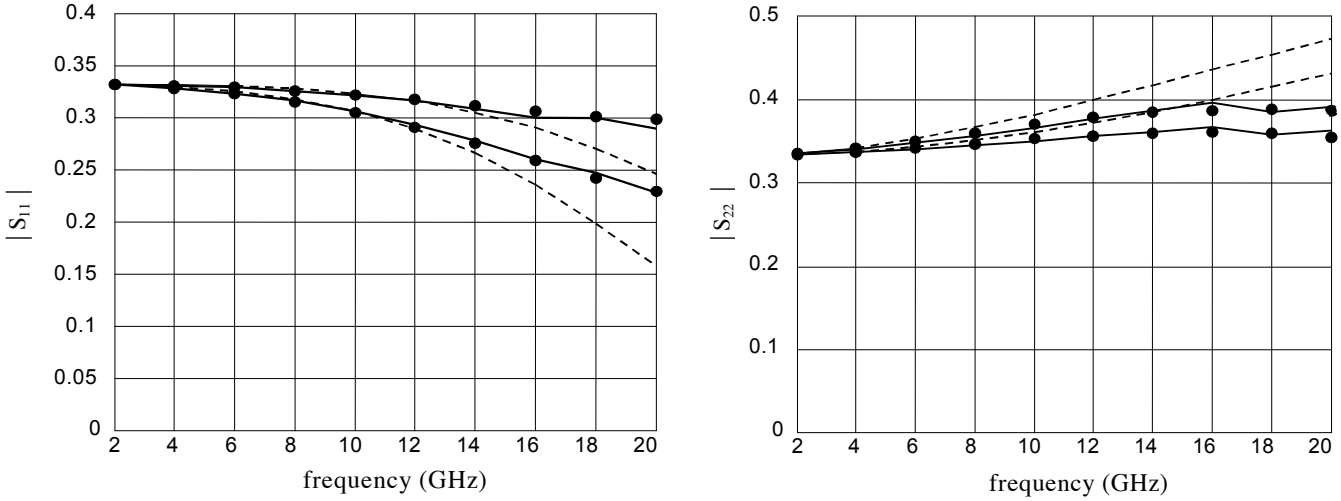

(a) (b)

Fig. 18. Responses of the shaped T-Junction at two test points in the region of interest by Sonnet's ***em*** (?), by the coarse model (---) and by the enhanced coarse model (?): (a) $|S_{11}|$; (b) $|S_{22}|$.

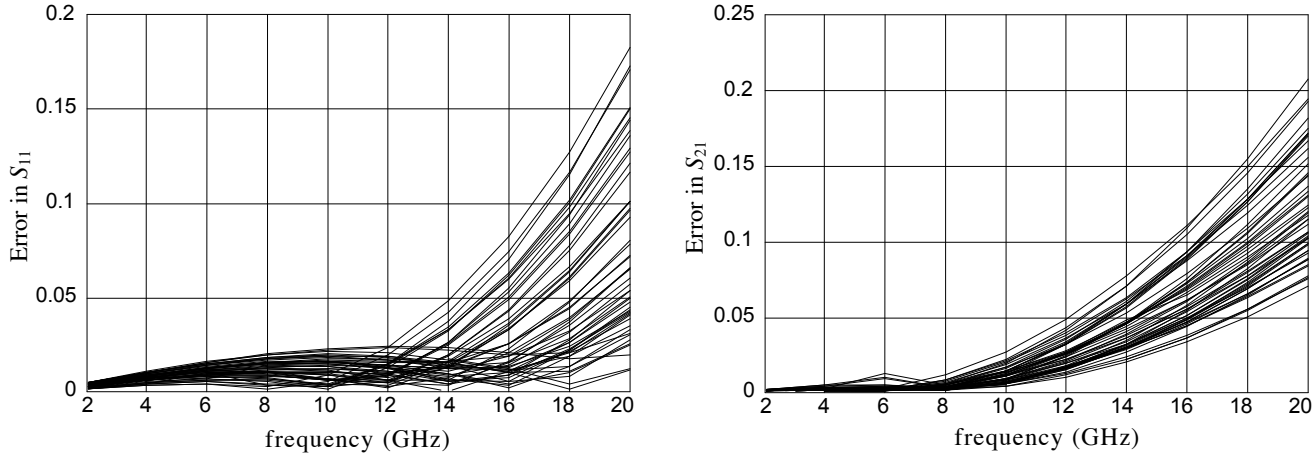

(a) (b)

Fig. 19. Error of the shaped T-Junction coarse model with respect to ***em***™: (a) in S_{11}; (b) in S_{22}.

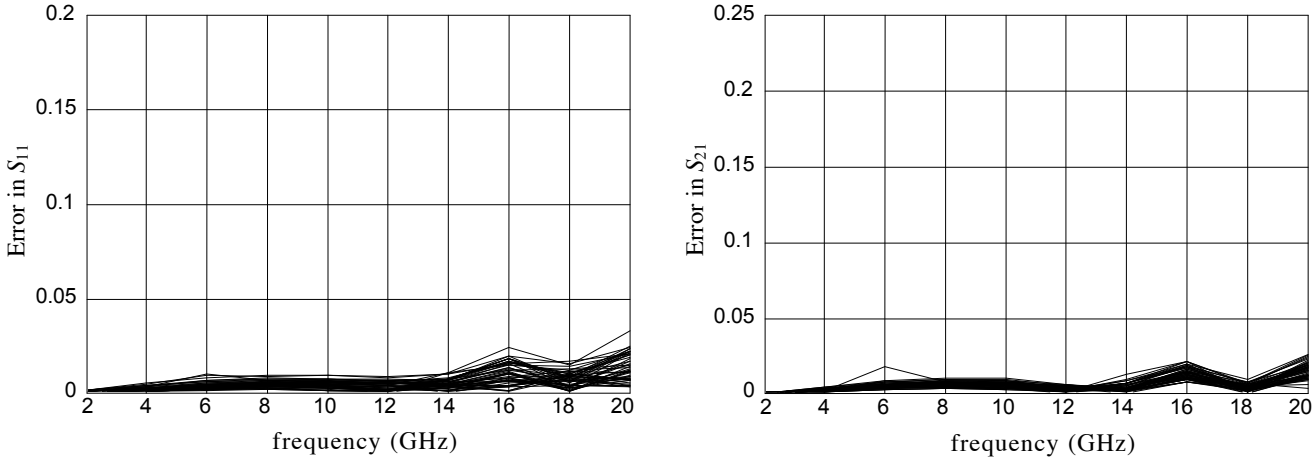

(a) (b)

Fig. 20. Error of the shaped T-Junction enhanced coarse model with respect to ***em***™: (a) in S_{11}; (b) in S_{22}.

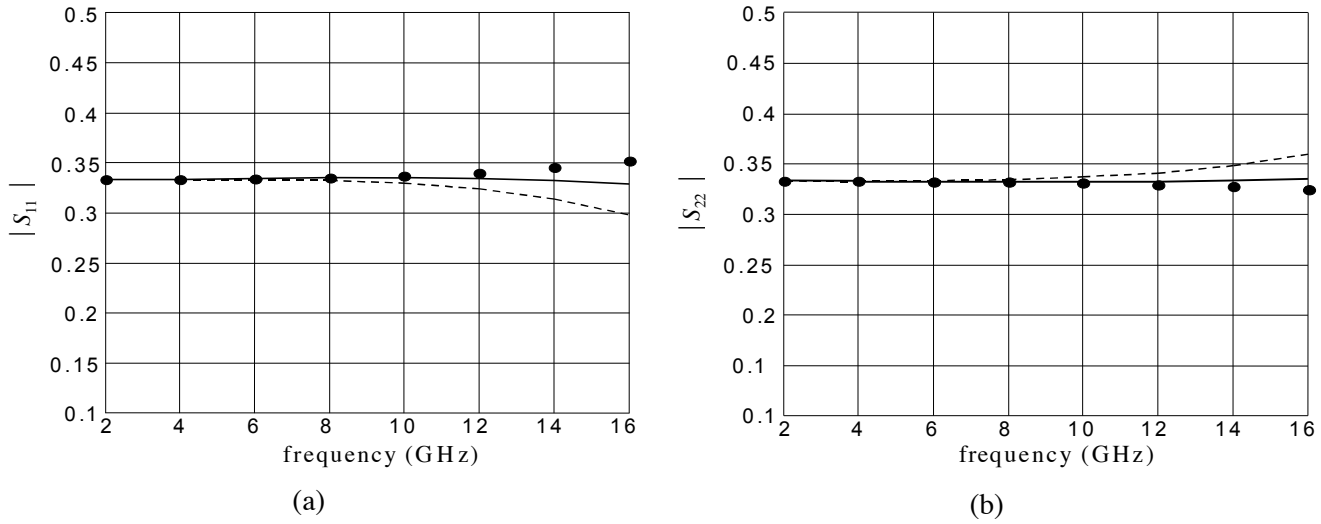

(a) (b)

Fig. 21. Responses of the optimum shaped T-Junction by Sonnet's ***em*** (?), by the coarse model (---) and by the enhanced coarse model (?): (a) $|S_{11}|$; (b) $|S_{22}|$.